Research Square

Preprints are preliminary reports that have not undergone peer review.
They should not be considered conclusive, used to inform clinical practice,
or referenced by the media as validated information.

Potentiality of bioactive compounds as inhibitor of M protein and F protein function of human respiratory syncytial virus

Debanjan Mitra (debanjanmitra267@gmail.com)
Raiganj University
Manish Paul
Maharaja Sriram Chandra Bhanja Deo University
Hrudayanath Thatoi
Maharaja Sriram Chandra Bhanja Deo University
Pradeep K. Das Mohapatra
Raiganj University

Research Article

Keywords: Human respiratory syncytial virus (RSV), Alnus japonica (Thunb.) Steud., Matrix protein, Fusion glycoprotein, Praecoxin A, Molecular dynamics simulation

Posted Date: August 30th, 2023

DOI: https://doi.org/10.21203/rs.3.rs-3295920/v1

License: This work is licensed under a Creative Commons Attribution 4.0 International License. Read Full License

Additional Declarations: No competing interests reported.

Version of Record: A version of this preprint was published at In Silico Pharmacology on December 24th, 2023. See the published version at https://doi.org/10.1007/s40203-023-00178-w.

Abstract

Context

The human respiratory syncytial virus (RSV) creates a pandemic every year in the European country. Lack of target therapeutics and absence of vaccines have prompted scientists to create novel vaccines or small chemical treatments against RSV's numerous targets. The matrix (M) protein and fusion (F) glycoprotein of RSV are well characterized and attractive drug targets. Five bioactive compounds from *Alnus japonica* (Thunb.) *Steud*. were taken into consideration as lead compounds. Drug-likeness characters of them showed the drugs are non-toxic and non-mutagenic and mostly lipophobic. Molecular docking reveals that all bioactive compounds have better binding and better inhibitory effect than ribavirin which is currently used against RSV. Praecoxin A appeared as the best lead compound between them. It creates 7 different types of bonds with amino acids of M protein and 5 different types of bonds with amino acids of F protein. Van der Waals interactions highly influenced the binding energies. Molecular dynamic simulations represent the non-deviated and less fluctuating nature of praecoxin A. Principal Component Analysis showed praecoxin A complex with RSV matrix protein is more stable than ribavirin complex. This study will help to develop a new drug to inhibit RSV.

Methods

All ligands were minimized through semi-empirical PM3 process with MOPAC. Toxicity was tested by ProTox-II server. Molecular docking studies were carried out using AutoDock 4.2. Molecular dynamics simulations for 100ns were carried out through GROMACS 5.12 MD and GROMOS96 43a1 force field. The graphs were produced by GROMACS's XMGrace program.

Introduction

Viral diseases are normally very deadly for humans. Especially, the fearful effects of COVID-19 force us to think about all those viral diseases which have no vaccine. There are many viruses available on the earth, which are the main cause of death of people. Respiratory syncytial virus (RSV) is one of them. After the discovery in 1957, it continually showed life-threatening effects on humans [1]. Mainly the European countries especially the USA, UK are heavily affected every winter by RSV. Death during winter by RSV is highest in the high-income country (91%) followed by low-income countries (77%) and middle-income countries (70%) respectively [2]. Investigation on hospitalized children those were suffered from pneumonia revealed that RSV is the main causing organism. 43% of children were infected by RSV was reported latterly [3]. RSV is generally caused in 6–10 years children [4]. However, it can cause notable morbidity and mortality in older age people [5]. Till now, two subgroups were identified; RSV-A and RSV-B. RSV A has a higher severity rate than RSV B. RSV A can react with all types of antibodies [6]. Children with type B RSV rarely required ventilation support than type A. Less than 3 years old children can be infected extremely by RSV A independently [7].

RSV has a negative-sense single-strand RNA genome which is linear and 15000 bp in length. The genome is non-segmented and consists of 10 genes that encode 11 proteins. All genes are situated in an orderly manner i.e., NS1, NS2, N, P, M, SH, G, F, M2, L. RSV can’t create pandemic situations due to unable to perform antigenic shift or genetic reassortment [8]. Haider et al. (2017) had performed a time scale dependent on evolutionary analysis which revealed that the rate of nucleotide substitution of BA genotype was higher than BA9 lineage [9]. Matrix protein (M) of RSV plays a crucial role in viral assembly, nucleocytoplasmic trafficking and also inhibit the rate of transcription which is a key factor for RSV pathogenesis [10]. Normally, M protein triggers particles assembly of virus when it

forms oligomers to dimers [11]. Two heptad repeat regions were found within the F protein of RSV. These regions are the main materials to form trimers of alpha-helical hairpin structures [12]. F protein has two subunits, F1 and F2. F2 subunit plays an important role in the determination of host cell specificity [13]. Besides *in-vitro* and *in-vivo* analysis nowadays *in-silico* analysis also plays important role in proteomics investigation [14–16]. The mathematical model of RSV revealed the mechanism to loss of its infectivity [17]. Conserved regions on sequences of N, F, G protein were also identified by *in silico* analysis of amino acid variation [18].

Identification of drug compounds for RSV is very much important. However, an FDA-approved drug named Ribavirin has already been used in the treatment of RSV. But it does not save children and adults from its lethal effect [19–20]. Researchers are still engaging to find an effective drug. A drug bindable pocket was found in the interaction site of nucleocapsid protein and phosphoprotein. Residue F241 plays a crucial role in this pocket area [21]. TMC353121 showed its antiviral activity by inhibiting the fusion glycoprotein of RSV in a non-primate model [22]. Derivatives of imidazopyridine showed promising IC50 value during the investigation and appeared as anti-RSV drugs [23]. Four dendrimers and three linear cationic antiviral peptides were screened out by investigations to inhibit the proteins of RSV [24]. Small molecules like JNJ2408068 and VP14637 were identified as an inhibitor of RSV fusion protein [25].

Computational prediction of the drug by molecular docking and molecular dynamics simulations are playing an enormous role in drug discovery. During the infection of COVID-19 and RSV, it has proved its effectiveness and importance [26–27]. Computational studies on pyrethroids showed a glide score of -4.54 and it has interacted with two important residues i.e., LYS46 and HIS151 of a target protein of RSV [28]. Modeling studies of Dichloro-phenyl-benzotriazoles was indicated that it can work as an RSV entry inhibitor [29]. A group of researchers had reported a group of compounds that were sharing a common di-thiocarbamate moiety. These compounds target the zinc finger motif of M2-1 protein from RSV [30]. Zinc finger reactive compounds were showed very promising results in both *in-vitro* and *in silico* analysis [31]. Nowadays, bioactive compounds are heavily used in the treatment of many different diseases. Bioactive chemicals from medicinal plants have long been studied as chemotherapeutic drugs in biomedicine and natural product research. Much insilico analysis provides significant reports on the use of bioactive compounds in colorectal cancer, breast cancer, diabetes, viral disease, etc. [32–35].

In this study, five bioactive compounds i.e., gemin D, praecoxin A, platyphylloside, oregonoyl A and oregonoyl B from *Alnus japonica* (Thunb.) Steud. which is found in Japan, China, Korea, were taken into consideration [36]. Gemin D has already shown its therapeutic effect on HIV inhibition [37]. According to some findings, praecoxin A protects against oxidative stress by lowering lipid peroxidation, boosting antioxidant defenses, and protecting against CCl4-induced histopathological alterations [38]. In colon cancer and leukemic Cells, platyphylloside acts as an antiproliferative and induces Apoptosis [39]. Tung et al. (2010) reported that oregonoyl A and oregonoyl B have anti-influenza effects [40]. Still now, only one drug i.e., ribavirin is used in the treatment of RSV. However, its efficacy in terms of improving outcomes is debatable. The effectiveness of this drug in the treatment of RSV illness has yet to be established [41].

Material and methods

Retrieval of ligands and their optimization

All bioactive compounds (Fig. 1.) were retrieved from the PubChem database which is the largest drug database [42]. All structures were downloaded in SDF format. They were subjected to optimization in a semi-empirical (PM3)

process with MOPAC. An adequate approach for computing partial charges is required for accurate complex geometry and binding energy calculation [43–44].

Retrieved of target protein

Two types of protein from RSV were chosen for this study. Fusion (F) glycoprotein (PDB ID: 5EA4) and matrix protein (PDB ID: 2VQP) were taken into consideration. These proteins were already reported as a good target for drugs [45–46]. Both structures were downloaded in PDB format from the RCSB PDB database [47]. Structures were chosen based on their high resolutions. Nowadays, the paradigm of a single ligand targeting a single protein has been replaced with a single molecule targeting several proteins. It outperforms earlier medication targeting technologies [48–49].

Calculations of drug-likeness properties

Drug-likeness qualities including solubility, permeability, metabolic stability, and transporter activities are crucial for drug candidates' success. Oral bioavailability, metabolism, clearance, toxicity, and in vitro pharmacology are all affected by this property [50]. Lipinski rule of five plays a significant role in this field [51]. However, violations of this rule don’t conclude that those drugs can’t be used. Cause this rule is only applicable for oral drugs [52].

Preparation of protein, ligand and performing molecular docking

Analysis of pockets of target protein was identified by CASTp sever [53]. Ligands and proteins were converted to the PDBQT file with the help of AutoDock 4.2. [54]. Rotatable bonds were fixed, and polar hydrogens were added in the PDBQT file. Grid box dimension and grid space were used as earlier reports [26–27]. Molecular docking of those bioactive compounds was performed by AUTODOCK 4.2. Protein-ligand complex was formed by the help of PyMol [55].

Molecular dynamics simulations

The molecular dynamics simulation (MD) was performed using two complex structures of matrix protein-coupled to praecoxin A, matrix protein-coupled to ribavirin (currently used drug), and apoprotein. All MD simulations were run on an Intel Xeon Quad-Core W3530 2.8 8M 1366 Processor with a LINUX environment, using the GROMACS 5.12 MD [56] and GROMOS96 43a1 force field [57]. The three protein systems were solvated in a cubic box holding 30306, 30337, and 30339 SPC216 water molecules, respectively, with dimensions of 98.535 X 98.535 X 98.535 nm^3 [58]. To neutralize the net charge of the system for each complex, four water molecules were substituted with Na. The solvate box margins were kept at a distance of 1.0 nm from all protein atoms. The solvated systems were subjected to 3000 steps of energy reduction using the steepest descent method. Following the energy minimization, position limited MD simulations were utilized to equilibrate both minimized systems for 100 ps at 300 K temperature to keep system pressure and temperature constant. After equilibration, both systems were exposed to a final production run of 100 ns MD simulations at 300 K temperatures. Periodic boundary conditions were applied using the Berendsen Coupling approach under isothermal and isobaric conditions, with relaxation durations of 0.1 and 0.2 ps, respectively [59]. The bond length was restricted in both systems using the LINCS technique with a time step of 2 fs [60]. The electrostatic interactions were studied using the Particle Mesh Ewald technique. With a cutoff of 1.0 nm, van der Waals and coulombic interactions were computed [61]. The MD trajectories were analyzed using the GROMACS software package's tools, such as RMSD and RMSF. The graphs were created using the XMGrace [62] software in GROMACS.

Principle component analysis

PCA or essential dynamics (ED) were used to assess the covariance matrices of the positional variations of C atoms, as well as the quantitative characterization of protein dynamism [63–64]. For both proteins, the first ten eigenvectors were good enough to examine. The ED approach was based on constructing the covariance matrix of the simulated proteins' coordinate variations. The eigenvectors and eigenvalues of the covariance matrix were diagonalized to get information on correlated movements throughout the protein. The MD simulation trajectories were utilized to construct the dynamics picture of the protein-ligand interface and relevant interactions using the Chimera visualization tool.

Results and Discussion

Evaluation of drug-likeness properties

According to Lipinski rule of five, for oral drugs, the molecular weight of a drug compound should be less than 500 Dalton. Hydrogen bond acceptor (HBA) and hydrogen bond donor (HBD) of oral drugs must be less than equal to 10 and 5, respectively. Octanol-water partition coefficient or LogP of drugs always maintains a value less than + 5. Violations of this rule indicate their delivery method should be injectable.

Only platyphylloside obey the Lipinski rule of five like ribavirin. So, it can be used as an oral drug. Other bioactive compounds show their injectable nature for drug delivery. Praecoxin A shows the highest molecular weight between them. Drugs more than 500 Dalton are not permeable to the skin and blood vessels [65]. Gemin D shows hydrophilic nature like ribavirin as they show negative LogP value. Other bioactive compounds show positive LogP value i.e., they are lipophilic. Lipophilic drugs have tended to diffuse across membranes in adipose tissue and muscle. Hydrophobicity and lipophilicity are significant features for different ways to forecast solubility, but they're also noteworthy from a pharmacological standpoint. Because drug molecules must cross the lipid bilayer of most cellular membranes, including those of enterocytes, the lipophilicity of drug candidate molecules is a critical consideration in the creation of its dosage form. As a result, it is widely assumed that medication molecules must be lipophilic to be well absorbed [66]. The combined surface area of oxygen and nitrogen atoms, as well as hydrogen atoms linked to these electronegative atoms, is known as the polar surface area (PSA) [67]. PSA has been proven to boost cellular potency, intestinal absorption, and blood-brain barrier penetration or limitation to the peripheral circulation when taken into account [68]. PSA shows the highest value in praecoxin A and lowest in platyphylloside between those bioactive compounds. Currently used drug also shows very lower value like platyphylloside. Hydrogen bond donor (HBD) and hydrogen bond acceptor (HBA) also show a higher number in praecoxin A. Bioavailability and binding potency are influenced by the number of rotatable bonds. The lower number of rotatable bonds increases the bioavailability of praecoxin A. So, it proves that praecoxin A is a better drug than other bioactive compounds. Praecoxin A possesses the highest ovality between all of them. It's also been claimed that ovality greater than 1.45 isn't mutagenic [69]. So, all those bioactive compounds of this study are non-mutagenic.

Analysis of pockets of target proteins

Pockets of proteins are playing an enormous role in drug design and discovery. A binding pocket is a hollow on the surface or within a protein that has the right characteristics for binding a ligand. A binding pocket's physicochemical properties are determined by the amino acid residues around it, which, along with its shape and position in a protein, establish its functioning [70]. Pockets larger than 20 $Å^2$ were considered for ligand binding sites. Matrix protein showed (Fig. 2.) 7 pockets with a large pocket area of 76.893 $Å^2$ and the lowest area of 20.936

$Å^2$. Fusion glycoprotein showed 12 pockets. The largest pocket area was 70.899 $Å^2$ and the lowest was 20.245 $Å^2$. Total 60 and 109 amino acids were participated in forming the pockets in matrix protein and F glycoprotein respectively. Mostly, polar residues were contributed more to this formation. Matrix protein showed 65% and F glycoprotein showed 62.38% polar residues in their pockets. So, polar residues have a major role formation of ligand binding pockets.

Molecular docking of bioactive compounds

Molecular docking analysis on those bioactive compounds shows their high binding with target proteins. Results were also compared with the currently used drug ribavirin. The result shows bioactive compounds are more effective than ribavirin in the treatment of RSV.

Praecoxin A showed the highest binding energies in both targets of RSV followed by oregonoyl B, oregonoyl A, gemin D, and platyphylloside. It showed − 13.8 Kcal/mol and − 13.3 Kcal/mol binding energies with matrix protein and F glycoprotein respectively. Oregonoyl B appeared as the second-best lead compound in this study. The binding energies with matrix protein and F glycoprotein were − 11.2 Kcal/mol and − 10.0 Kcal/mol, respectively. Ribavirin showed the lowest score for each bioactive compound. Praecoxin A showed (Fig. 3.) 2 conventional hydrogen bonds, 1 pi-cation, 1 pi-anion, 1 pi-donor hydrogen bond, 1 unfavorable accepter-accepter bond, 1 unfavorable donor-donor bond, and 7 Van der Waals interactions in binding with matrix protein. In the case of F glycoprotein, it creates 1 conventional hydrogen bond, 3 pi-alkyl bonds, 1 pi donor hydrogen bond, 2 unfavorable positive-positive bonds, and 16 Van der Waals interactions. Unfavorable positive-positive interaction was found between LYS315 and two oxygen atoms of a benzene ring. However, unfavorable interaction does not arise questions on the performance of that drug. Because of protein flexibility, modeling frequently fails. FDA-approved drugs can be used in other treatments. Many previous reports prescribed drugs with unfavorable interaction [71–72]. Oregonoyl B showed 1 carbon-hydrogen bond with 2 conventional hydrogen bonds, 1 pi-cation bond, and 9 Van der Waals interactions to inhibit RSV matrix protein (Fig. 4.). To inhibit the F glycoprotein of RSV, oregonoyl B creates 1 pi-sigma, 1 alkyl, 1 pi-alkyl, 1 pi-hydrogen 10 Van der Waal bonds. Also, it formed an unfavorable donor-donor with Asp194. Oregonoyl A formed 5 conventional hydrogen bonds, 2 pi-alkyl, and 7 Van der Waal interactions in molecular docking with matrix protein. 4 conventional hydrogen bond, 2 pi-sigma bond, 1 carbon-hydrogen bond, 1 unfavorable acceptor-acceptor bond, and 5 Van der Waals interactions were formed in interaction with F glycoprotein. Gemin D created 1 pi-pi T shaped bond, 2 pi-alkyl bond, 1 pi-donor hydrogen bond, and 9 Van der Waals interaction to inhibit matrix protein, whereas 1 conventional hydrogen bond, 1 pi-cation bond, 2 pi-alkyl bond, 1 carbon-hydrogen bond, 1 unfavorable donor-donor bond and 10 Van der Waals interactions were formed in interaction with F glycoprotein. Platyphylloside formed 2 conventional hydrogen bonds, 2 pi-cation bonds, 1 alkyl bond, and 11 Van der Waals interactions to inhibit matrix protein of RSV. In the case of F glycoprotein, its formed 2 pi-cation, 3 pi-alkyl, 1 unfavorable donor-donor interaction, and 13 Van der Waals interactions. Lys193 of matrix protein of RSV created many bonds with praecoxin A, oregonoyl B, and platyphylloside. Thr239 from similar proteins also contributed to forming a bond in every drug (except gemin D). It creates a conventional hydrogen bond with drugs (in the case of platyphylloside it created Van der Waal). In F glycoprotein and drug interactions, Lys315, His317, Arg339 have participated to create bonds with every drug except oregonoyl B.

Molecular dynamic simulations

Root mean square deviation

The root-mean-square deviation (RMSD) is a commonly used measure of the discrepancies between predicted and observed values (sample or population values) by a model or estimator. Other non-protein molecules, such as tiny chemical compounds, can be calculated using the RMSD method. During the simulation time, this computation may quantify the spatial differences between the backbone atoms present in the protein. The differences are determined concerning the starting structure of the simulation. The smaller the discrepancies, the more geographically equivalent to compared structures are, whereas the RMSD values of structures that are more distantly connected are substantially bigger. From the comparative RMSD study of matrix protein-coupled to praecoxin A, matrix protein-coupled to ribavirin and apoprotein it can be reported that praecoxin A complex shows greater deviation than apoprotein and ribavirin bound complex at starting to 15ns. After that, it was astonishingly noticed that praecoxin A complex shows almost the same pattern as apoprotein (Fig. 5a). But complex with ribavirin shows very high deviation than apoprotein and praecoxin A bound complex. It was noted that the overall average values for apoprotein and praecoxin A bound complex were around between 0.25 and 0.30nm. RMSD analysis on those complexes in comparison to apoprotein indicates that praecoxin A bound complex is more stable than ribavirin bound complex. According to the results of the RMSD calculation evaluated from the MD simulation, Paul et al. (2014) found that thermophilic chemotaxis linked protein CheY is more stable than its mesophilic cousin [56].

Root mean square fluctuation

The root means square fluctuation (RMSF) is a measurement of a single atom's (or a group of atoms') displacement from the reference structure, average over the number of atoms [73]. The graph of RMSF derived for the Cα atoms relative to the average structure during the simulation provides a more thorough perspective of variations in residue mobility in matrix protein linked to praecoxin A, matrix protein-coupled to ribavirin, and apoprotein. RMSF values rise as a protein's secondary structure is depleted, which can be caused by a decrease in binding affinity between the protein and the ligand. Praecoxin A bound complex showed very lower fluctuation than ribavirin complex and apoprotein (Fig. 5b). At position 70, praecoxin A showed the highest fluctuation in its total path. This study suggested that the complex with praecoxin A has comparatively more stability than the ribavirin complex.

Radius of gyration

The radius of gyration is described as the root-mean-square average of all scattering elements' distance from the molecule's center of mass. The radius of gyration (Rg) is a measurement of the compactness and size of protein molecules. It's about how frequent secondary structures may be compactly integrated into a protein's 3D structure [74]. Praecoxin A complex displayed the lowest radius of gyration than ribavirin complex and apoprotein (Fig. 6a). The lower radius of gyration indicates its high tightest packing. After, 4000ps or 40ns all three studied protein complexes starting deviate. Praecoxin A complex and ribavirin complex go downward whereas apoprotein goes upward. The summary of this result indicates that the protein is more tightly packed and stable with praecoxin A.

Solvent accessible surface area

Proteins' solvent-accessible surface area (SASA) is an important factor in influencing their folding and stability. SASA is calculated from protein structures using various methods, as well as protein sequences using machine-learning techniques trained on solved structures. It is described as the surface characterized surrounding a protein by the van der Waals contact surface of the molecule and a hypothetical center of a solvent sphere. A protein's amino acid residues can be classed as buried or exposed based on SASA values. During the simulation, apoprotein

and ribavirin showed a very identical pattern of SASA values (Fig. 6b). A lower SASA value is usually linked with a better folding process, and atoms' accessible surface areas are related to their hydrophobicity [75]. Praecoxin A showed a moderate decrease value than others which implies that the folding mechanism in the praecoxin A complex structure was more efficient than in other structures.

Principle component analysis

Principal Component Analysis (PCA) is a sophisticated statistical approach that uses a decomposition procedure to filter observed movements from the biggest to smallest spatial scales to systematically minimize the number of dimensions required to characterize protein dynamics [76]. In normal modes analysis, these prominent movements correspond to associated vibrational modes or collective motions of groups of atoms. By comparing distinct drug-protein complexes, any structural quality change during molecular dynamics simulation may be identified using this approach. Analysis was done against two eigenvectors i.e., 1 and 2. PCA analysis demonstrated that praecoxin A complex structure is more congested or closely clouded than apoprotein and ribavirin complex (Fig. 7). According to the 2D map, apoprotein shows flexibility with an eigenvalue of -12 to + 10 and ribavirin shows flexibility with an eigenvalue of -10 to + 11, whereas praecoxin A complex represents the lowest flexibility with an eigenvalue of -6 to + 7. The above result demonstrated that the praecoxin A complex is more stable than the apoprotein and ribavirin-protein complex.

Conclusion

Since there is no RSV vaccine, it is necessary to create effective and focused measures to combat the disease. By focusing on the matrix protein and F glycoprotein, we investigated the therapeutic nature of 5 bioactive compounds from the *Alnus japonica* (Thunb.) Steud. The present in silico analysis shows that praecoxin A, which has been approved by the FDA, might be used as antiviral medicine for the treatment of RSV. Comparative analysis concerning the currently used drug ribavirin, its indicated that praecoxin is A better drug to inhibit the RSV. It shows almost double binding energy than ribavirin. Drug likeness properties indicate the injectable nature of praecoxin A. This molecule was further selected for molecular dynamics simulations. Molecular dynamics simulations showed that the stability of protein complex with praecoxin A is better than ribavirin complex. The radius of gyration reported that protein with praecoxin A is more tightly packed than others. Using various in-vitro and in-vivo experiments, the plant bioactive compound praecoxin A, or other bioactive compounds, may be examined for its inhibitory activity against RSV. Furthermore, the backbone structure of praecoxin A might be used to generate more effective RSV inhibitors.

Declarations

Acknowledgement

The authors are grateful to Bioinformatics Facility, Department of Biotechnology, Maharaja Sriram Chandra Bhanja Deo University, Baripada, India, for the provision of computational support. The work was partially conducted in the context of the Bioinformatics Resources and Applications Facility (BRAF), C-DAC, Pune, India.

Ethical Approval

NA

Competing interests

Authors declared that they have no conflict of interest.

Authors' contributions

D.M. conceived and designed the project. P.K.D.M. conducted initial manual verifications. Target protein and ligand compounds were identified by D.M. Molecular docking was performed by D.M. Molecular dynamic simulations were performed by M.P and H.T. Analysis of those results was done by D.M. Draft of the manuscript was prepared by D.M and M.P. Final version of the manuscript was edited by H.T. The whole work was done under the supervision of P.K.D.M.

Funding

None

Availability of data and materials

NA

References

1. Chanock RO, Roizman BE (1957) Recovery from infants with respiratory illness of a virus related to chimpanzee coryza agent (CCA). I. Isolation, properties and characterization. Am J Hyg 66:281–290
2. Scheltema NM, Gentile A, Lucion F et al (2017) Global respiratory syncytial virus-associated mortality in young children (RSV GOLD): a retrospective case series. Lancet Glob Health 5:e984–e991
3. Wang Y, Ji W, Chen Z et al (2014) Comparison of severe pneumonia caused by Human metapneumovirus and respiratory syncytial virus in hospitalized children. Indian J Pathol Microbiol 57(3):413
4. Kolawole MB, Gobir G, Abdulkadri AA (2017) Serological Survey of Respiratory Syncytial Virus (RSV) Among Children in Lorin North-Central, Nigeria. Pakistan J Med Dentistry 6(4):3–10
5. Allen KE, Beekmann SE, Polgreen P, Poser S, Pierre JS, Santibañez S, Gerber SI, Kim L (2018) Survey of diagnostic testing for respiratory syncytial virus (RSV) in adults: infectious disease physician practices and implications for burden estimates. Diagn Microbiol Infect Dis 92(3):206–209
6. Walsh EE, McConnochie KM, Long CE, Hall CB (1997) Severity of respiratory syncytial virus infection is related to virus strain. J Infect Dis 175(4):814–820
7. Mufson MA, Örvell C, Rafnar B, Norrby E (1985) Two distinct subtypes of human respiratory syncytial virus. J Gen Virol 66(10):2111–2124
8. Mitra D, Das Mohapatra PK (2023) In silico comparative structural and compositional analysis of glycoproteins of RSV to study the nature of stability and transmissibility of RSV A. Syst Microbiol Biomanufacturing 3(2):312–327
9. Haider MS, Khan WH, Deeba F, Ali S, Ahmed A, Naqvi IH, Dohare R, Alsenaidy HA, Alsenaidy AM, Broor S, Parveen S (2018) BA9 lineage of respiratory syncytial virus from across the globe and its evolutionary dynamics. PLoS ONE 13(4):e0193525
10. Ghildyal R, Ho A, Jans DA (2006) Central role of the respiratory syncytial virus matrix protein in infection. FEMS Microbiol Rev 30(5):692–705

11. Förster A, Maertens GN, Farrell PJ, Bajorek M (2015) Dimerization of matrix protein is required for budding of respiratory syncytial virus. J Virol 89(8):4624–4635
12. Zhao X, Singh M, Malashkevich VN, Kim PS (2000) Structural characterization of the human respiratory syncytial virus fusion protein core. Proceedings of the National Academy of Sciences. ;97(26):14172-7
13. Schlender J, Zimmer G, Herrler G, Conzelmann KK (2003) Respiratory syncytial virus (RSV) fusion protein subunit F2, not attachment protein G, determines the specificity of RSV infection. J Virol 77(8):4609–4616
14. Mitra D, Mohapatra PK (2021) Cold adaptation strategy of psychrophilic bacteria: an in-silico analysis of isocitrate dehydrogenase. Syst Microbiol Biomanufacturing. :1–1
15. Mitra D, Pal AK, Das Mohapatra PK (2022) Intra-protein interactions of SARS-CoV-2 and SARS: a bioinformatic analysis for plausible explanation regarding stability, divergency, and severity. Syst Microbiol Biomanufacturing 2(4):653–664
16. Mitra D, Mohapatra PK (2021) Discovery of Novel Cyclic Salt Bridge in Thermophilic Bacterial Protease and Study of its Sequence and Structure. Appl Biochem Biotechnol 193(6):1688–1700
17. Beauchemin CA, Kim YI, Yu Q, Ciaramella G, DeVincenzo JP (2019) Uncovering critical properties of the human respiratory syncytial virus by combining in vitro assays and in silico analyses. PLoS ONE 14(4):e0214708
18. Souza C, Zanchin NI, Krieger MA, Ludwig A (2017) In silico analysis of amino acid variation in human respiratory syncytial virus: insights into immunodiagnostics. Memórias do Instituto Oswaldo Cruz 112:655–663
19. Committee on Infectious Diseases (1993) Use of ribavirin in the treatment of respiratory syncytial virus infection. Pediatrics 92(3):501–504
20. Groothuis JR, Woodin KA, Katz R, Robertson AD, McBride JT, Hall CB, McWilliams BC, Lauer BA (1990) Early ribavirin treatment of respiratory syncytial viral infection in high-risk children. J Pediatr 117(5):792–798
21. Ouizougun-Oubari M, Pereira N, Tarus B, Galloux M, Lassoued S, Fix J, Tortorici MA, Hoos S, Baron B, England P, Desmaële D (2015) A druggable pocket at the nucleocapsid/phosphoprotein interaction site of human respiratory syncytial virus. J Virol 89(21):11129–11143
22. Ouizougun-Oubari M, Pereira N, Tarus B, Galloux M, Lassoued S, Fix J, Tortorici MA, Hoos S, Baron B, England P, Desmaële D (2015) A druggable pocket at the nucleocapsid/phosphoprotein interaction site of human respiratory syncytial virus. J Virol 89(21):11129–11143
23. Feng S, Hong D, Wang B, Zheng X, Miao K, Wang L, Yun H, Gao L, Zhao S, Shen HC (2015) Discovery of imidazopyridine derivatives as highly potent respiratory syncytial virus fusion inhibitors. ACS Med Chem Lett 6(3):359–362
24. Kozhikhova KV, Shilovskiy IP, Shatilov AA, Timofeeva AV, Turetskiy EA, Vishniakova LI, Nikolskii AA, Barvinskaya ED, Karthikeyan S, Smirnov VV, Kudlay DA (2020) Linear and dendrimeric antiviral peptides: Design, chemical synthesis and activity against human respiratory syncytial virus. J Mater Chem B 8(13):2607–2617
25. Douglas JL, Panis ML, Ho E, Lin KY, Krawczyk SH, Grant DM, Cai R, Swaminathan S, Chen X, Cihlar T (2005) Small molecules VP-14637 and JNJ-2408068 inhibit respiratory syncytial virus fusion by similar mechanisms. Antimicrob Agents Chemother 49(6):2460–2466
26. Mitra D, Paul M, Thatoi H, Mohapatra PK (2021) Study of potentiality of dexamethasone and its derivatives against Covid-19. J Biomol Struct Dynamics 16:1–1
27. Mitra D, Mohapatra PK (2022) Effect of natural compounds to inhibit human respiratory syncytial virus. Smart Environ Sci Technol Manage. :97–101

28. Kant K, Rangra NK, Behera PC, Bani B, Dey S, Lal UR, Mishra AN, Ghosh M Computational prediction of pyrethroids as promising agents against respiratory syncytial virus: a comparative study
29. Piras S, Sanna G, Carta A, Corona P, Ibba R, Loddo R, Madeddu S, Caria P, Aulic S, Laurini E, Fermeglia M (2019) Dichloro-phenyl-benzotriazoles: A new selective class of human respiratory syncytial virus entry inhibitors. Front Chem 7:247
30. Cancellieri M, Bassetto M, Widjaja I, van Kuppeveld F, de Haan CA, Brancale A (2015) In silico structure-based design and synthesis of novel anti-RSV compounds. Antiviral Res 122:46–50
31. Boukhvalova MS, Prince GA, Blanco JC (2010) Inactivation of respiratory syncytial virus by zinc finger reactive compounds. Virol J 7(1):1–0
32. Mitra D, Dey A, Biswas I, Das Mohapatra PK (2021) Bioactive compounds as a potential inhibitor of colorectal cancer; an insilico study of Gallic acid and Pyrogallol. Annals of Colorectal Research 9(1):32–39
33. Djati S (2021) Anti-breast cancer potential activity of Phaleria macrocarpa (Scheff.) Boerl. leaf extract through in silico studies. J Pharm Pharmacognosy Res 9(6):824–845
34. Zainab B, Ayaz Z, Alwahibi MS, Khan S, Rizwana H, Soliman DW, Alawaad A, Abbasi AM (2020) In-silico elucidation of Moringa oleifera phytochemicals against diabetes mellitus. Saudi J Biol Sci 27(9):2299–2307
35. Setlur AS, Naik SY, Skariyachan S (2017) Herbal lead as ideal bioactive compounds against probable drug targets of Ebola virus in comparison with known chemical analogue: A computational drug discovery perspective. Interdisciplinary Sciences: Computational Life Sciences 9(2):254–277
36. Sati SC, Sati N, Sati OP (2011) Bioactive constituents and medicinal importance of genus Alnus. Pharmacogn Rev 5(10):174
37. Nakashima H, Murakami T, Yamamoto N, Sakagami H, Tanuma SI, Hatano T, Yoshida T, Okuda T (1992) Inhibition of human immunodeficiency viral replication by tannins and related compounds. Antiviral Res 18(1):91–103
38. Al-Sayed E, Abdel-Daim MM, Khattab MA (2019) Hepatoprotective activity of praecoxin A isolated from Melaleuca ericifolia against carbon tetrachloride-induced hepatotoxicity in mice. Impact on oxidative stress, inflammation, and apoptosis. Phytother Res 33(2):461–470
39. Lee JE, Thuy NT, Lee J, Cho N, Yoo HM (2019) Platyphylloside isolated from betulaplatyphylla is antiproliferative and induces apoptosis in colon cancer and leukemic cells. Molecules 24(16):2960
40. Tung NH, Kwon HJ, Kim JH, Ra JC, Ding Y, Kim JA, Kim YH (2010) Anti-influenza diarylheptanoids from the bark of Alnus japonica. Bioorg Med Chem Lett 20(3):1000–1003
41. Saravolatz LD, Empey KM, Peebles RS Jr, Kolls JK (2010) Pharmacologic advances in the treatment and prevention of respiratory syncytial virus. Clin Infect Dis 50(9):1258–1267
42. Kim S, Thiessen PA, Bolton EE, Chen J, Fu G, Gindulyte A, Han L, He J, He S, Shoemaker BA, Wang J (2016) PubChem substance and compound databases. Nucleic Acids Res 44(D1):D1202–D1213
43. Stewart JJ (1990) MOPAC: a semiempirical molecular orbital program. J Comput Aided Mol Des 4(1):1–03
44. Pedretti A, Mazzolari A, Vistoli G (2008) VEGA ZZ: a versatile toolkit for drug design and protein modelling. InCongreso de FisicoquímicaTeórica y Computacional
45. Costello M, Ray HC, Chaiwatpongsakorn W, E Peeples S (2012) Targeting RSV with vaccines and small molecule drugs. Infectious Disorders-Drug Targets (Formerly Current Drug Targets-Infectious Disorders). 12(2):110–128

46. Bharaj P, Wang YE, Dawes BE, Yun TE, Park A, Yen B, Basler CF, Freiberg AN, Lee B, Rajsbaum R (2016) The matrix protein of Nipah virus targets the E3-ubiquitin ligase TRIM6 to inhibit the IKKε kinase-mediated type-I IFN antiviral response. PLoS Pathog 12(9):e1005880
47. Kouranov A, Xie L, de la Cruz J, Chen L, Westbrook J, Bourne PE, Berman HM (2006) The RCSB PDB information portal for structural genomics. Nucleic Acids Res 34(suppl1):D302–305
48. Zhang W, Pei J, Lai L (2017) Computational multitarget drug design. J Chem Inf Model 57(3):403–412
49. Kumar A, Tiwari A, Sharma A (2018) Changing paradigm from one target one ligand towards multi-target directed ligand design for key drug targets of Alzheimer disease: an important role of in silico methods in multi-target directed ligands design. Curr Neuropharmacol 16(6):726–739
50. Di L, Kerns EH, Carter GT (2009) Drug-like property concepts in pharmaceutical design. Curr Pharm Design 15(19):2184–2194
51. Lipinski CA (2004) Lead-and drug-like compounds: the rule-of-five revolution. Drug discovery today: Technologies 1(4):337–341
52. Benet LZ, Hosey CM, Ursu O, Oprea TI (2016) BDDCS, the rule of 5 and drugability. Adv Drug Deliv Rev 101:89–98
53. Tian W, Chen C, Lei X, Zhao J, Liang J (2018) CASTp 3.0: computed atlas of surface topography of proteins. Nucleic Acids Res 46(W1):W363–W367
54. Forli W, Halliday S, Belew R, Olson AJ (2012) AutoDock Version 4.2. J Med Chem 55(2):623–638
55. DeLano WL, Pymol (2002) An open-source molecular graphics tool. CCP4 Newsletter on protein crystallography. 40(1):82–92
56. Paul M, Hazra M, Barman A, Hazra S (2014) Comparative molecular dynamics simulation studies for determining factors contributing to the thermostability of chemotaxis protein CheY. J Biomol Struct Dynamics 32(6):928–949
57. van Gunsteren WF, Billeter SR, Eising AA, Hünenberger PH, Krüger PK, Mark AE, Scott WR, Tironi IG (1996) Biomolecular simulation: the GROMOS96 manual and user guide. VdfHochschulverlag AG an der ETH Zürich, Zürich. ;86:1–044
58. Miyamoto S, Kollman PA (1992) Molecular dynamics studies of calixspherand complexes with alkali metal cations: calculation of the absolute and relative free energies of binding of cations to a calixspherand. J Am Chem Soc 114(10):3668–3674
59. Weber W, Hünenberger PH, McCammon JA (2000) Molecular dynamics simulations of a polyalanine octapeptide under Ewald boundary conditions: influence of artificial periodicity on peptide conformation. J Phys Chem B 104(15):3668–3675
60. Hess B, Bekker H, Berendsen HJ, Fraaije JG (1997) LINCS: a linear constraint solver for molecular simulations. J Comput Chem 18(12):1463–1472
61. Darden T, Perera L, Li L, Pedersen L (1999) New tricks for modelers from the crystallography toolkit: the particle mesh Ewald algorithm and its use in nucleic acid simulations. Structure 7(3):R55–60
62. Vaught A (1996) Graphing with Gnuplot and Xmgr: two graphing packages available under linux. Linux J 1996(28es):7–es
63. Amadei A, Ceruso MA, Di Nola A (1999) On the convergence of the conformational coordinates basis set obtained by the essential dynamics analysis of proteins' molecular dynamics simulations. Proteins Struct Funct Bioinform 36(4):419–424

64. Amadei A, Linssen AB, Berendsen HJ (1993) Essential dynamics of proteins. Proteins Struct Funct Bioinform 17(4):412–425
65. Bos JD, Meinardi MM (2000) The 500 Dalton rule for the skin penetration of chemical compounds and drugs. Experimental Dermatology: Viewpoint 9(3):165–169
66. Zhu L, Lu L, Wang S, Wu J, Shi J, Yan T, Xie C, Li Q, Hu M, Liu Z Oral absorption basics: pathways and physicochemical and biological factors affecting absorption. InDeveloping solid oral dosage forms 2017 (pp. 297–329). Academic Press
67. Schaftenaar G, de Vlieg J (2012) Quantum mechanical polar surface area. J Comput Aided Mol Des 26(3):311–318
68. Clark DE (2011) What has polar surface area ever done for drug discovery? Future Med Chem 3(4):469–484
69. Lucas MC, Bhagirath N, Chiao E, Goldstein DM, Hermann JC, Hsu PY, Kirchner S, Kennedy-Smith JJ, Kuglstatter A, Lukacs C, Menke J (2014) Using ovality to predict nonmutagenic, orally efficacious pyridazine amides as cell specific spleen tyrosine kinase inhibitors. J Med Chem 57(6):2683–2691
70. Stank A, Kokh DB, Fuller JC, Wade RC (2016) Protein binding pocket dynamics. Acc Chem Res 49(5):809–815
71. Dhorajiwala TM, Halder ST, Samant L (2019) Comparative in silico molecular docking analysis of l-threonine-3-dehydrogenase, a protein target against African trypanosomiasis using selected phytochemicals. J Appl Biotechnol Rep 6(3):101–108
72. Ibrahim ZY, Uzairu A, Shallangwa G, Abechi S (2020) Molecular docking studies, drug-likeness and in-silico ADMET prediction of some novel β-Amino alcohol grafted 1, 4, 5-trisubstituted 1, 2, 3-triazoles derivatives as elevators of p53 protein levels. Sci Afr 10:e00570
73. Mitra D, Das Mohapatra PK Computational Intelligence in Identification of Some FDA Approved Drug Compounds for Treatment of COVID-19. InArtificial Intelligence and Machine Learning Methods in COVID-19 and Related Health Diseases 2022 Jun 29 (pp. 109–122). Cham: Springer International Publishing
74. Mitra D, Afreen S, Das Mohapatra PK, Abdalla M (2023) Threat of respiratory syncytial virus infection knocking the door: a proposed potential drug candidate through molecular dynamics simulations, a future alternative. J Mol Model 29(4):91
75. Veno J, Rahman RN, Masomian M, Ali MS, Kamarudin NH (2019) Insight into improved thermostability of cold-adapted staphylococcal lipase by glycine to cysteine mutation. Molecules 24(17):3169
76. David CC, Jacobs DJ Principal component analysis: a method for determining the essential dynamics of proteins. InProtein dynamics 2014 (pp. 193–226). Humana Press, Totowa, NJ

Tables

Table 1
Drug-likeness properties of gemin D, praecoxin A, platyphylloside, oregonoyl A and oregonoyl B in compare with Ribavirin.

Name	PubChem ID	M.W (Daltons)	LogP	Polar Surface Area (PSA) Å²	HBD	HBA	Rotatable bond	Volume (Å³)	Ovality
Gemin D	471119	634.46	-0.2	318.49	11	18	6	491.21	1.87
Praecoxin A	14777390	952.6	1.3	464	16	27	3	715.2	1.9778
Platyphylloside	9826264	476.52	1.2	157	6	9	11	431.45	1.799
Oregonoyl A	44602673	624.6	2.8	203	7	12	14	549.43	1.9217
Oregonoyl B	44602674	654.7	2.8	213	7	13	15	574.98	1.9701
Ribavirin	37542	244.2	-1.8	144	4	7	3	197.68	1.5098

Table 2
Binding energies with target protein of gemin D, praecoxin A, platyphylloside, oregonoyl A and oregonoyl B in compare with Ribavirin

Name	Matrix protein (2VQP) Kcal/mol	F glycoprotein (5EA4) Kcal/mol
Gemin D	-10.3	-9.9
Praecoxin A	-13.8	-12.7
Platyphylloside	-10.1	-9.2
Oregonoyl A	-10.5	-10.0
Oregonoyl B	-11.2	-10.0
Ribavirin	-6.7	-6.1

Figures

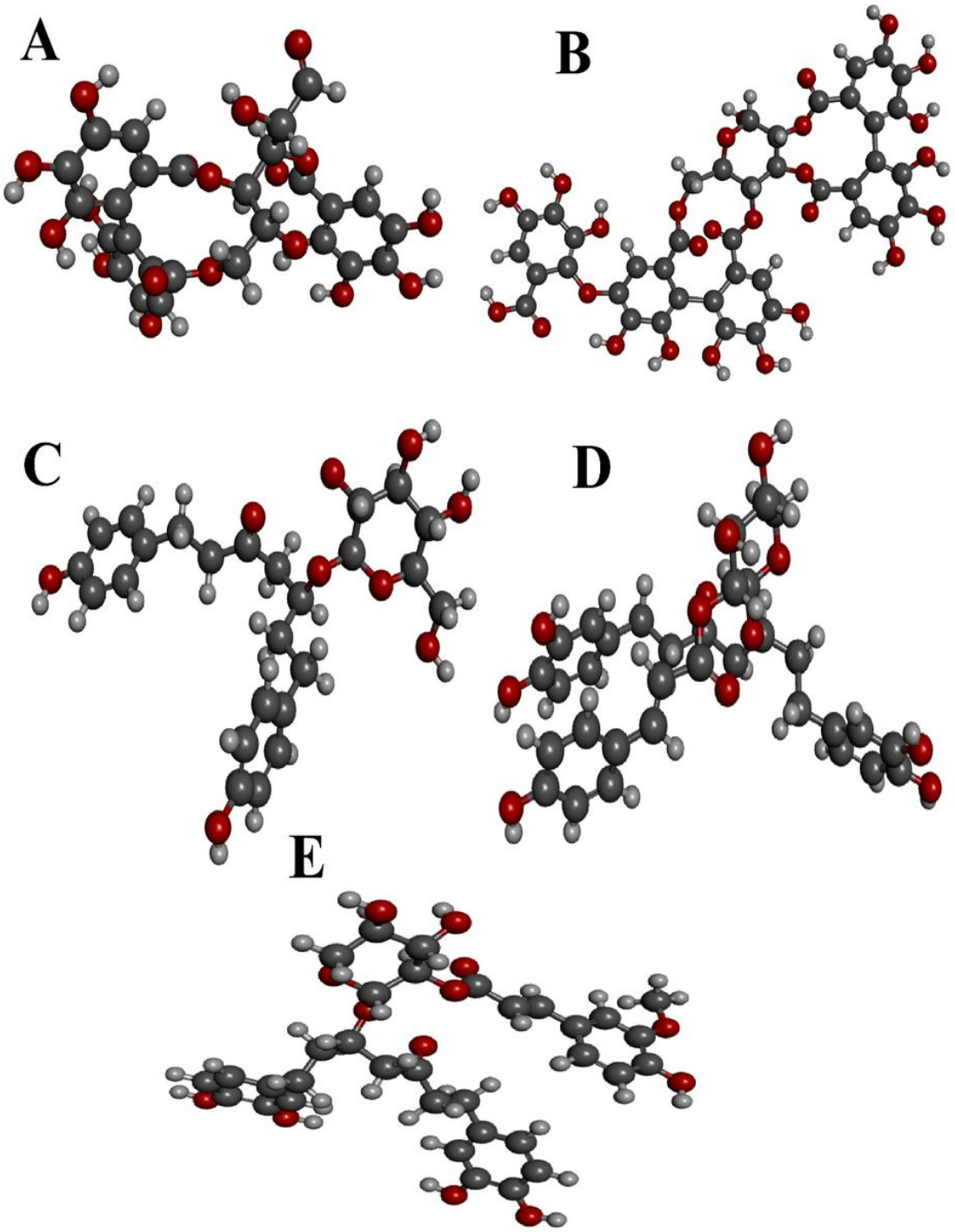


Figure 1

3D structures of bioactive compounds gemin D, praecoxin A, platyphylloside, oregonoyl A and oregonoyl B.

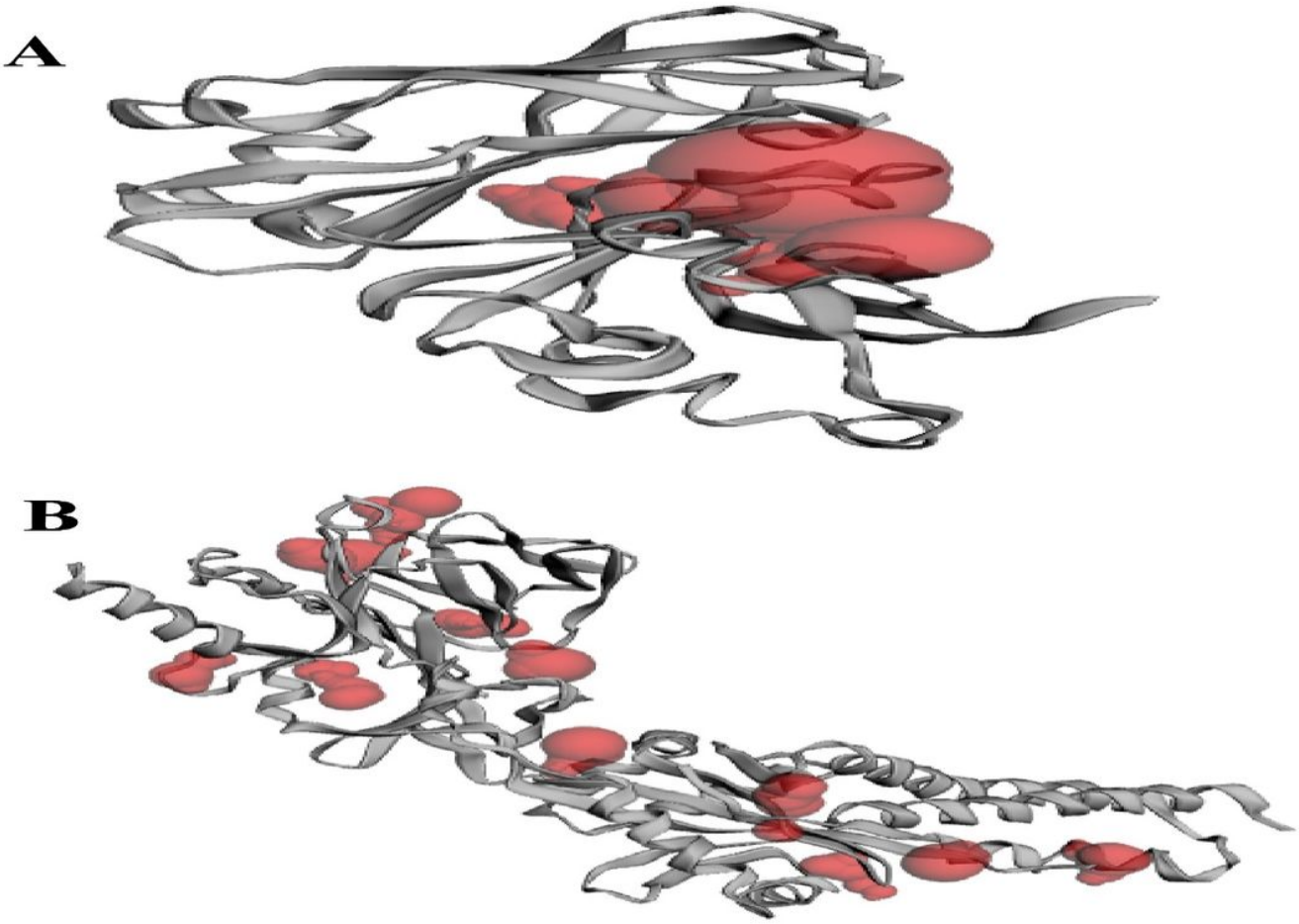


Figure 2

Pockets in matrix protein (PDB ID: 2VQP) and F glycoprotein (PDB ID: 5EA4).

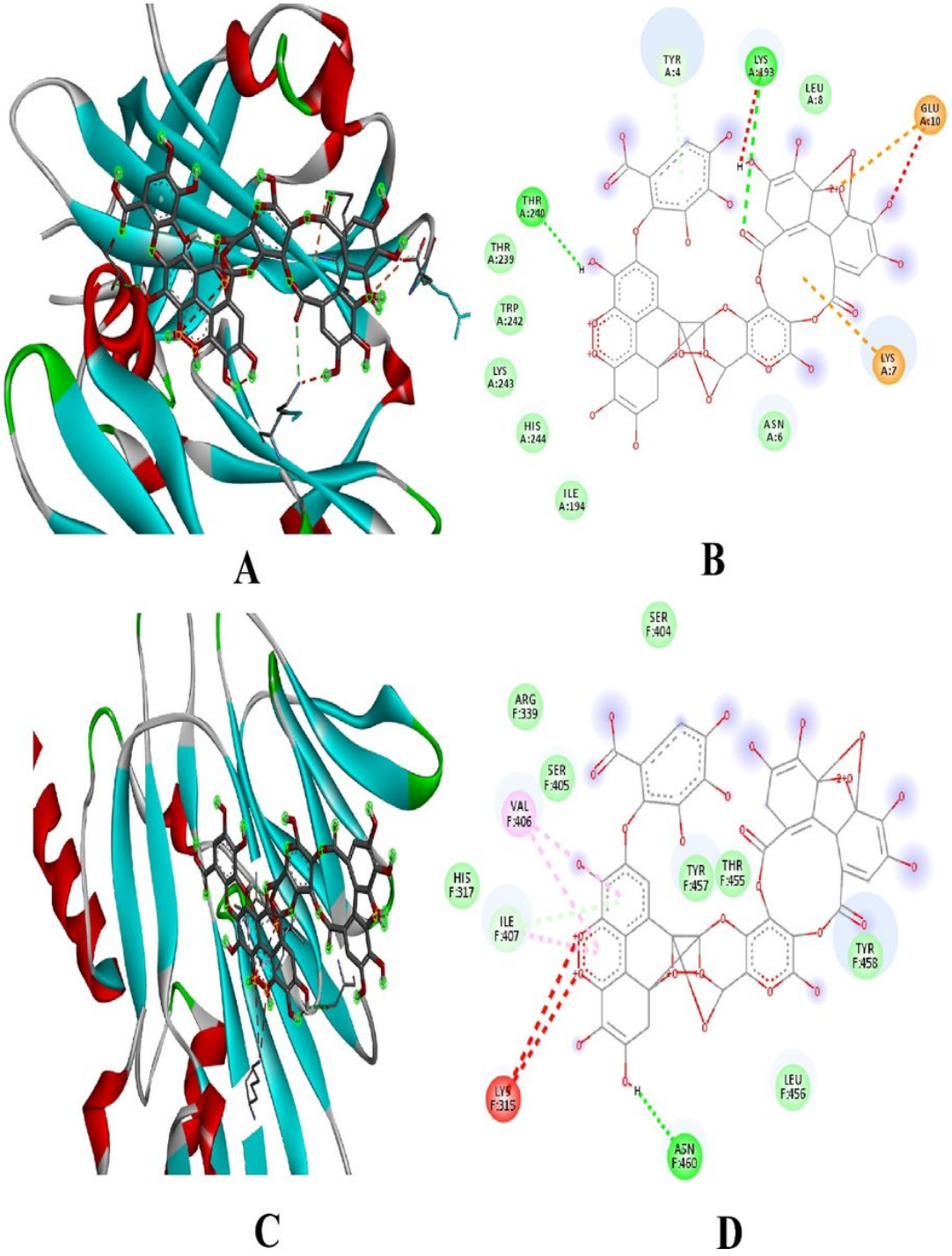


Figure 3

A. 3D interaction of praecoxin A with matrix protein B. 2D interaction of praecoxin A with matrix protein showing ligand-amino acid interaction C. 3D interaction of praecoxin. A with F glycoprotein D. 2D interaction of praecoxin A with F glycoprotein showing ligand-amino acid interaction

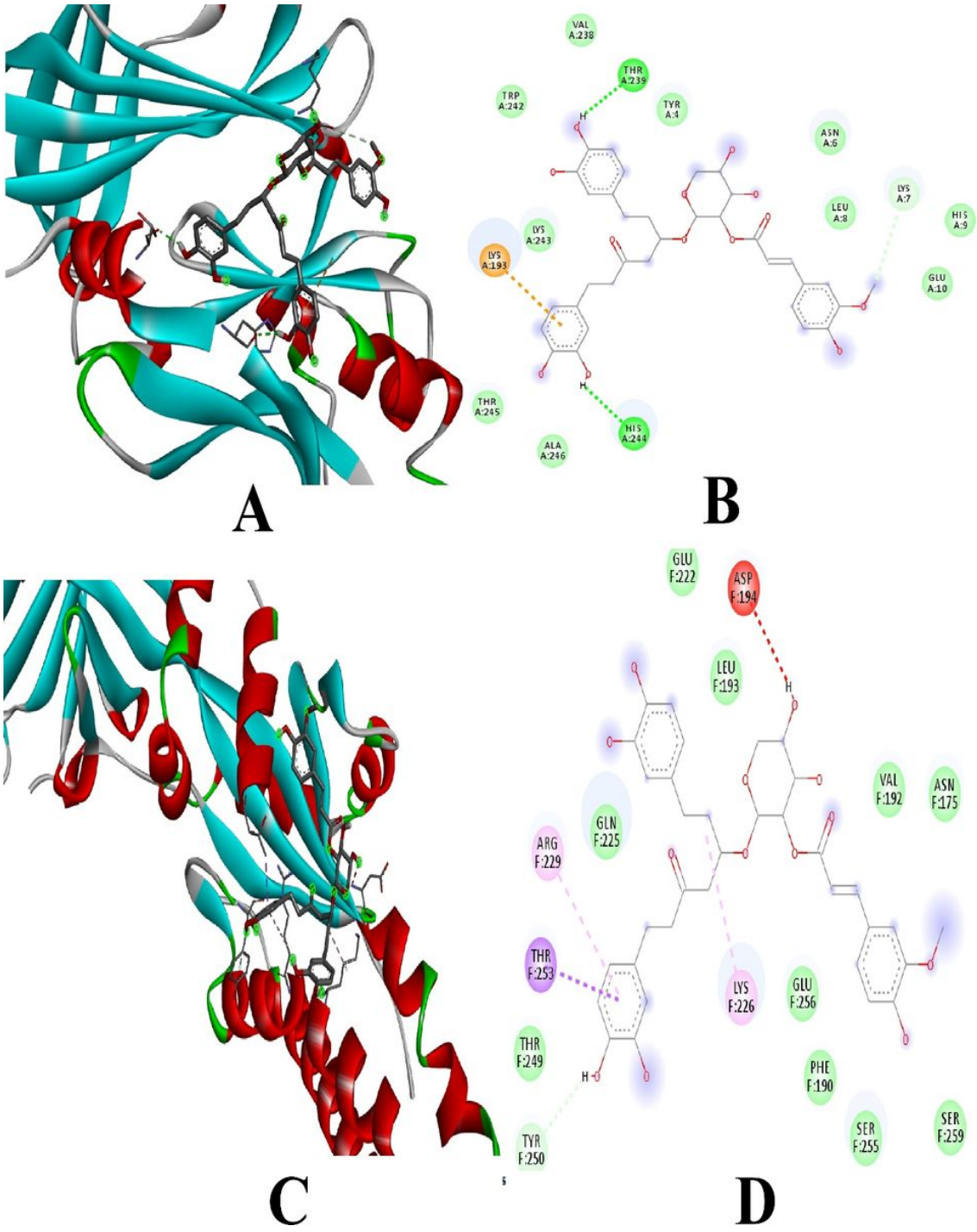


Figure 4

A. 3D interaction of oregonoyl B with matrix protein B. 2D interaction of oregonoyl B with matrix protein showing ligand-amino acid interaction C. 3D interaction of oregonoyl B with F glycoprotein D. 2D interaction of oregonoyl B with F glycoprotein showing ligand-amino acid interaction.

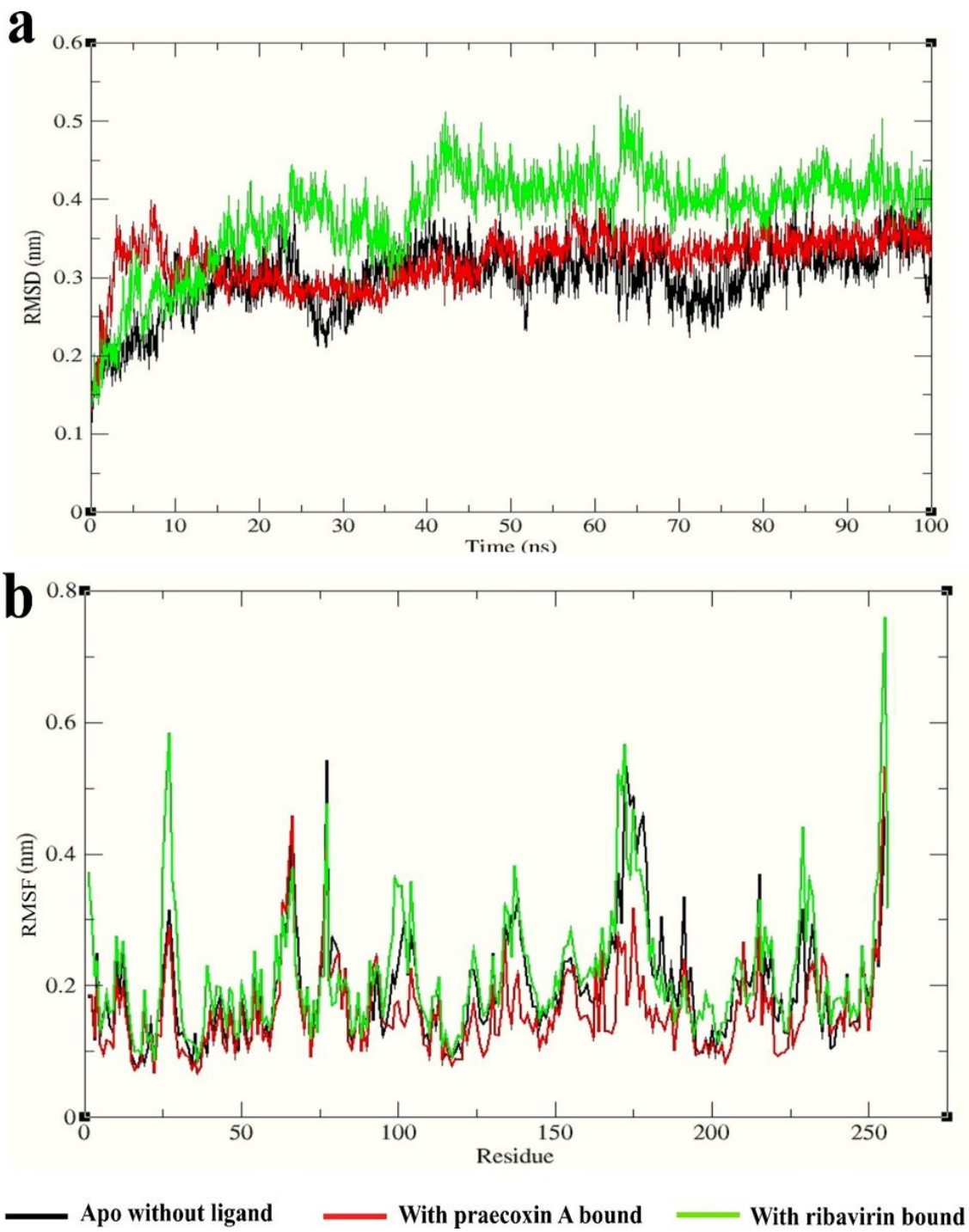


Figure 5

a. RMSD of apoprotein, praecoxin A complex, ribavirin complex in 100ns showing their structural deviation b. RMSF of apoprotein, praecoxin A complex, ribavirin complex in 100ns showing the fluctuation with respect to residues number.

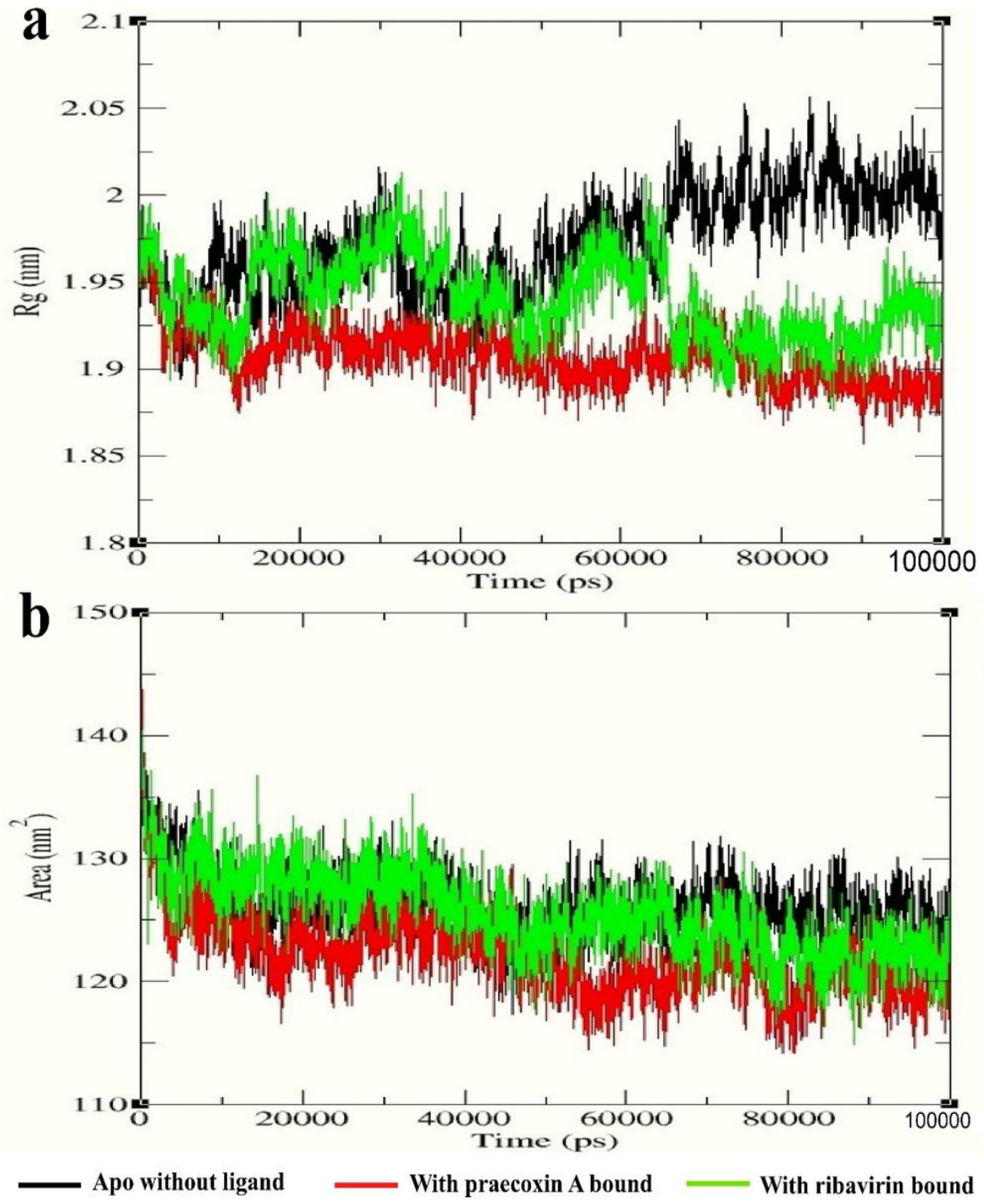


Figure 6

Radius of gyration (Rg) of apoprotein, praecoxin A complex, ribavirin complex in 10000ps showed protein packing quality b. Solvent accessible surface area of apoprotein, praecoxin A complex, ribavirin complex showing their folding mechanism.

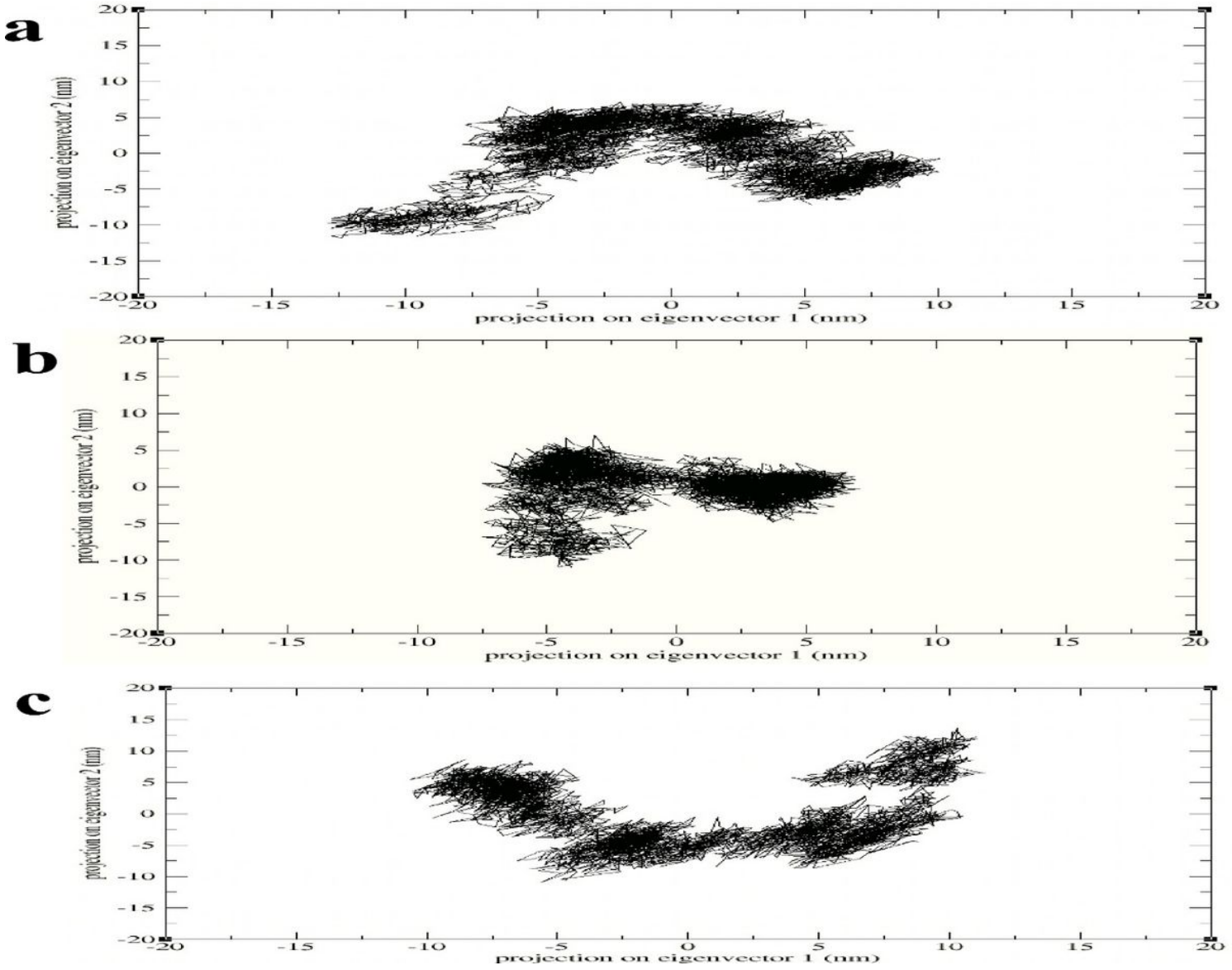


Figure 7

Principal Component Analysis (PCA) of a. apoprotein, b. praecoxin A complex, c. ribavirin complex against two eigenvectors showed better stability of praecoxin A complex.